Author's version
published in IEEE/ASME Transactions on Mechatronics vol 20, no 3, pp 1384-1394, June 2015
doi: 10.1109/TMECH.2014.2337514.

Actuator with Angle-Dependent Elasticity for Biomimetic Transfemoral Prostheses

Serge Pfeifer, Anna Pagel, *Student Member, IEEE,* Robert Riener, *Member, IEEE,* and Heike Vallery, *Member, IEEE*

***Abstract*—Despite tremendous improvements in recent years, lower-limb prostheses are still inferior to their biological counterparts. Most powered knee joints use impedance control, but it is unknown which impedance profiles are needed to replicate physiological behavior. Recently, we have developed a method to quantify such profiles from conventional gait data. Based on this method, we derive stiffness requirements for knee prostheses, and we propose an actuation concept where physical actuator stiffness changes in function of joint angle. The idea is to express stiffness and moment requirements as functions of angle, and then to combine a Series Elastic Actuator (SEA) with an optimized nonlinear transmission and parallel springs to reproduce the profiles. By considering the angle-dependent stiffness requirement, the upper bound for the impedance in zero-force control could be reduced by a factor of two. We realize this ANGle-dependent ELAstic Actuator (ANGELAA) in a leg, with rubber cords as series elastic elements. Hysteresis in the rubber is accounted for, and knee moment is estimated with a mean error of 0.7 Nm. The nonlinear parallel elasticity creates equilibria near 0° as well as 90° knee flexion, frequent postures in daily life. Experimental evaluation in a test setup shows force control bandwidth around 5-9 Hz, and a pilot experiment with an amputee subject shows the feasibility of the approach. While weight and power consumption are not optimized in this prototype, the incorporated mechatronic principles may pave the way for cheaper and lighter actuators in artificial legs and in other applications where stiffness requirements depend on kinematic configuration.**

***Index Terms*—Series Elastic Actuation, Force Control, Prosthetics, Variable Stiffness, Viscoelasticity**

Manuscript submitted December 28, 2013; revised March 11, 2014 and May 08, 2014. This work was supported by the ETH Research Grant ETHIIRA, the Gottfried und Julia Bangerter-Rhyner Stiftung and the Swiss National Science Foundation through the National Centre of Competence in Research Robotics.

S. Pfeifer, A. Pagel and R. Riener are with the Sensory-Motor Systems Lab, ETH Zurich and Medical Faculty, University of Zurich, Switzerland (email: pfeifers@ethz.ch; pagela@ethz.ch; riener@hest.ethz.ch). H. Vallery is with the Department of BioMechanical Engineering, Delft University of Technology, 2628 CD Delft, The Netherlands and the Sensory-Motor Systems Lab, ETH Zurich (email: h.vallery@tudelft.nl).

Corresponding author: Heike Vallery, 3ME, TU Delft, 2628CD Delft, NL. h.vallery@tudelft.nl, Phone: +31 15-27 83517.

I. Introduction

MECHATRONIC technology to replace human legs after amputation has made major advances over the past 15 years. In particular, the advent of knee joints with microprocessor-controlled damping, like the C-Leg (Otto Bock, Duderstadt, Germany), significantly improved mobility and reduced the incidence of falls in transfemoral amputees [1]. However, these artificial legs are still inferior to their physiological counterparts in that they can only dissipate mechanical energy. As a result, the gait of unilateral transfemoral amputees is asymmetric [2], and tasks where able-bodied subjects heavily rely on positive knee joint power, such as stair climbing with alternating legs, require considerable adaptation of the motor pattern [3].

To remedy this problem, powered knee prostheses have been presented in recent years by various research groups [4]–[7] and one company (the PowerKnee from Össur, Reykjavik, Iceland). Often, variable-impedance controllers are employed, which detect the gait phase from a finite set of phases and apply different impedance parameters for each phase [4]–[6]. Another trend is to develop controllers that resemble physiological control mechanisms of the joints, such as artificial reflexes [8]. For both concepts, strategies for automatic parameter tuning for different locomotor tasks and gait phases have been suggested [9], [10]. However, it is unknown in how far the obtained impedance profiles reproduce biological function, as quantitative data on physiological knee joint impedance during gait is still missing.

Following the assumption that knowledge of physiological impedance could facilitate control design, several research groups are currently working on quantifying physiological joint impedance during gait using special apparatus that apply perturbations [11]–[13]. It is known that one major determinant of joint impedance is short-range stiffness of biological muscle [14], which describes differential changes in muscles force in response to differential changes in muscle length. Via kinematic transformation, this property governs how the moment that muscles generate about a joint responds to

differential changes in joint angle. It is not to be confused with the quasi-stiffness often used to describe [15] or replicate [16] the apparent covariation of joint angle and moment during gait.

Recently, we presented a model-based method to estimate physiological knee stiffness only from conventional kinematic, kinetic, and electrophysiological recordings [17]. This method enables us to estimate stiffness profiles during diverse activities, for example level-ground gait, stair ascent, or stair descent, without applying perturbations. With this information, we can precisely define hardware requirements for a prosthetic device that can replicate physiological behavior, not only in terms of moment generation and velocity, as commonly done for powered prostheses, but also in terms of stiffness.

To allow the replication of the estimated physiological stiffness templates, a prosthetic device needs to be able to modulate its apparent stiffness in a wide range. Existing knee prostheses mostly use stiff, high-bandwidth actuators [5], [7], [18]. While stiff actuators are ideal for high-stiffness applications, because of their high bandwidth and high positioning precision [19], a compliant element in series with the motor improves force control performance to allow rendering of low impedances [20], protects the transmission mechanically from impacts [21], makes devices safer to interact with humans [22], and has the potential for energy storage [23], properties that are all desired in prosthetic applications. Actuator units that can vary their physical stiffness combine the advantages of stiff and compliant actuation [24]–[27], and have therefore already been used in a knee prosthesis [4]. However, mechanisms to arbitrarily vary physical stiffness require a second actuator, and, hence, increase weight and complexity, which is undesired in prosthetic applications. Furthermore, none of these actuators were designed to replicate intrinsic stiffness profiles of a biological joint.

In this paper, we propose a new variant of Series (Visco-)Elastic Actuator (SVA), where a nonlinear transmission changes the actuator stiffness in function of joint angle. Because the benefits of a Series Elastic Actuator (SEA) are most apparent when stiffness is minimal (guided by the design constraints), we minimize stiffness while still being able to replicate physiological behavior. To this end, we derive explicit nonlinear requirements from physiology using our model-based stiffness analysis of biomechanical data. Instead of metal springs, which are commonly used as series-elastic elements in such devices [4], [28], the concept relies on rubber cords. In addition, the concept also incorporates parallel springs that were positioned such that in combination with the actuator, the asymmetric moment-angle profile of a physiological joint is approximated. The device is named ANGELAA (ANGle-dependent ELAstic Actuator). An observer accurately estimates force from deflection despite hysteresis in the rubber. We evaluated the performance of the device in a test setup and in a pilot experiment with an amputee subject walking with a prosthesis prototype.

II. Methods

A. Requirements for Biomimetic Behavior

We assumed that ideal prosthetic knee joint hardware should match the capabilities of a physiological knee as closely as possible. Hence, we aimed to design an actuation mechanism that is capable of replicating biological function in terms of knee moment, velocity, and stiffness, which we consider to be the key functional determinants in combination with weight and mass distribution of the leg. The device should serve as a tethered test platform for different control strategies for transfemoral prostheses, so energy consumption is secondary.

Moment and power requirements of a prosthetic knee joint are often deducted from normative gait data from unimpaired subjects (e.g. [29], [30]). Alternatively, assuming a powered knee joint was used in combination with a passive ankle, knee data from below-knee amputees fitted with a passive ankle prosthesis could be used as a reference [31], [32]. During the same activity, the discrepancy in knee moment between unimpaired subjects and below-knee amputees is substantial. For example in stair ascent, peak moment is around 80 Nm for unimpaired subjects [30], and 15 Nm for below-knee amputees [31]. Hence, it is difficult to deduct requirements for a powered knee prosthesis from these data, especially when it is unclear whether the knee will be used in combination with a passive or a powered ankle. To obtain more generic requirements that are independent of a specific activity or prosthetic foot, we looked at the peak performance characteristics of a physiological knee joint instead.

Moment and stiffness capabilities of a physiological knee strongly depend on knee angle. For moment capabilities, we used an empirical model [33] to obtain the relationship between peak moment and knee angle (Fig. 1). Here and in the following, we used a body mass of 75 kg and a height of 1.75 m as a base for our requirements.

To estimate physiological knee stiffness, we have developed a model-based approach that uses kinematic, kinetic and electromyographic (EMG) measurements during healthy human gait. We already validated this

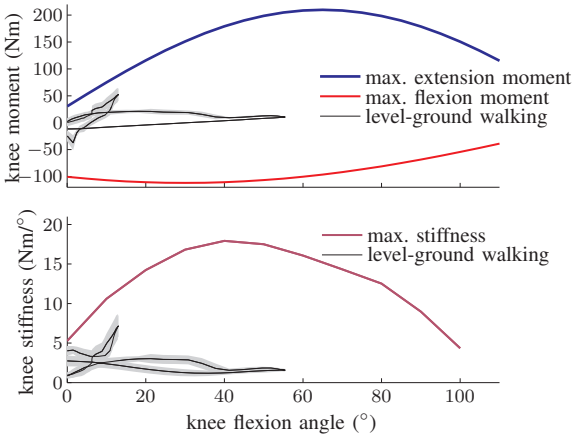

Fig. 1. Top: Peak physiological knee extension and flexion moments (at 100 % activation) as a function of knee angle, based on an empirical model [33], assuming a body mass of 75 kg and a height of 1.75 m. Bottom: Corresponding physiological knee stiffness estimated with our model-based approach to predict knee stiffness [17], assuming 50 % activation of both flexor and extensor muscles. For both quantities, moment and stiffness, mean (black solid line) and standard deviation (shaded area) over 10 gait cycles of an able-bodied subject (72 kg, 1.84 m) are shown for comparison (not used for optimization).

model by comparing it to perturbation responses under static conditions [17]. Using this model, we quantified peak physiological knee stiffness. We assumed that both flexor and extensor muscle groups are activated at 50 % of their maximum values (based on the peak moment profiles obtained as described above). This assumed activation pattern represents heavy co-contraction. The resulting peak stiffness-angle profile is shown in Fig. 1.

For peak velocity capabilities, the literature indicates that unloaded peak joint velocity is around 700 °/s [34], but it is unclear at which angles this can be achieved. Therefore, we also analyzed different locomotor activities, as recorded by Riener et al. [30], and we found maximum velocities of 320 °/s at 35° flexion angle for level-ground walking, 365 °/s at 52° for stair ascent, and 320 °/s at 55° for stair descent. Due to the less pronounced dependency between velocity and knee angle, we did not explicitly make the peak velocity requirement dependent on knee angle, but aimed to achieve the peak physiological velocity of 700 °/s over the entire range.

For peak power requirements, the model by Anderson et al. [33] suggests 460 W. For comparison, during physiological stair ascent, peak power amounts to 190 W in physiological stair ascent, and -300 W in descent [30].

B. Hardware Design

Human joint movements are low-speed and high-torque applications compared to suitably sized electric motors. A high transmission ratio is necessary to realize the required joint torques. Commonly, Harmonic Drive gears [35] or ball-screw mechanisms are employed to this end [18], [36]. We selected a ball screw mechanism due to its better back-driveability and higher efficiency compared to Harmonic Drive gears [35], [37]. At a comparable transmission ratio, ball screws also offer a slight weight advantage [38].

The use of a ball screw makes transmission ratio a nonlinear function of joint angle. This is not a disadvantage for our application, but instead can be exploited to achieve moment-angle and stiffness-angle profiles that resemble physiological properties, which are also nonlinear.

Our proposed actuation concept is based on the idea of Series Elastic Actuators (SEAs), which means that the ball screw is connected to the shank via elastic elements. To translate knee stiffness requirements to design choices, we used the finding that the apparent stiffness a conventional SEA can display while maintaining passivity is bounded by the physical stiffness of the elastic elements [20]. Therefore, this physical stiffness, reflected on the knee joint, must be at least as high as the maximum required stiffness.

To meet the space constraints given by the envelope of a physiological shank, we aligned two pretensioned elastic elements with the shank, and connected them to the ball-screw over a rocker (Fig. 2). This concept also allows us to choose the ratio between the lengths of the two rocker lever arms r_1 and r_2 (Fig. 2) to configure the joint stiffness. This geometry, in combination with the ball screw attachment points, yields nonlinear moment-angle and stiffness-angle profiles, which can be tailored to mimic physiological profiles.

We selected a motor with high power density and low weight: a Maxon EC30 4-pole brushless motor (Maxon Motor AG, Sachseln, Switzerland) with 200 W nominal power output, which should satisfy the power requirements for stair ascent. As the motor can be overloaded for short periods, it should also be capable of providing the necessary negative power in stair descent, without the need for additional dissipative elements. It only weighs 300 g while providing a nominal output torque of 0.13 Nm, and a nominal speed of 15800 rpm. We combined the motor with a drive (Maxon EPOS3, Maxon Motor AG, Sachseln, Switzerland) and power supply that would allow peak torque of four times the nominal values (0.52 Nm). To enable such controlled overloading of the motor outside of its specified range, the motor was modified to incorporate two PT100 temperature sensors in its windings. The motor drives the ball-nut of the ball screw (diameter: 12 mm, lead: 5 mm, Eichenberger Gewinde AG, Burg, Switzerland) using a

timing-belt transmission (1:3). A detailed analysis on how this transmission was dimensioned can be found in [39].

All parameters describing the geometry (i.e. the attachment points of the elastic elements, the attachment points of the ball-screw transmission, the length, pivot point, and transmission ratio r_1/r_2 of the rocker element) are found by minimizing the following cost function:

$$J = \int_{\phi_{\min}}^{\phi_{\max}} [\tau_{\mathrm{e}}(\phi) - \tau_{\mathrm{e}}^*(\phi)]^2 + [\tau_{\mathrm{f}}(\phi) - \tau_{\mathrm{f}}^*(\phi)]^2 + \lambda \left[K(\phi) - K^*(\phi)\right]^2 \mathrm{d}\phi, \quad (1)$$

where τ, K represent peak physiological (targeted) joint torque and stiffness (Fig. 1), τ^*, K^* represent the approximated values by the actuator, and subscripts e, f indicate knee extension and flexion, respectively. The weighting factor was $\lambda = (23\,^\circ)^2$, and the integral limits $\phi_{\min} = 0^\circ$, $\phi_{\max} = 100^\circ$. The parameters were constrained such that the resulting design roughly fit in the outline of a human shank. Furthermore, the maximum lever arm of the linear actuator with respect to the knee joint was constrained, to ensure that the required joint velocities could be reached.

We used a grid optimization with a resolution of 10 mm for the ball-screw attachment points, and 5 mm for the spring attachment points and rocker pivot point. The rocker transmission r_1/r_2 was varied from 0.1 to 0.4 in steps of 0.05. Because it was not feasible to find a solution with the given motor, we relaxed the joint velocity requirement to 500 °/s. This value contains enough margin to be able to achieve the required velocities in physiological gait and stair negotiation. We ran the optimization with a pair of theoretical linear-elastic extension elements with a stiffness of 10 kN/m and a free length of 100 mm.

The force control performance of conventional actuators, including SEAs, can be improved by adding viscosity [40]–[42]. One effective way of adding viscosity without the need for additional viscous elements (which would increase overall weight) is to use visco-elastic elements instead of linear-elastic elements in the SEA, turning it into a Series Visco-Elastic Actuator (SVA). Viscoelastic polymers are also generally lighter than linear-elastic (steel) springs.

Therefore, we used rubber as elastic material in the final design: Two pairs of parallel rubber cords (J. G. Karl Schmidt GmbH & Co. KG, Solingen, Germany) take the role of the two theoretical elastic elements on either side of the rocker. Each cord has a diameter of 12 mm, a length of unstressed rubber of 40 mm, and a maximum deflection of 190 % of that length (76 mm). Neglecting hysteresis and nonlinearity, the combined stiffness of a pair of cords is approximately 7.3 kN/m in the main operating range. The pair of cords weighs 73 g, including the metal clamps for fixation. In comparison, a steel extension springs with similar stiffness (7.1 kN/m) and maximum deflection (72 mm), has a length of uncompressed spring body of 92 mm, an outer diameter of 25 mm, and it weighs 142 g (Gutekunst + Co.KG Spring Factories, Metzingen, Germany), so it consumes more space and weighs roughly twice as much as the rubber cords. The disadvantage of these viscoelastic properties in terms of hysteresis can be dealt with using an observer [42], as described in Section II-C, such that force can still be measured accurately.

To exploit the fact that the physiological knee is much stronger in extension than in flexion, springs acting in parallel to the actuation unit were added to the design (Fig. 2). Depending on the location of the spring attachment points (P and Q), the moment-angle profile can be very different (Fig. 3). For a set of off-the shelf extension springs, we optimized geometry to produce a maximal extension moment near 60° flexion, while having only little contribution near full extension and 90° flexion, frequent postures in daily life. The cost function was

$$J = \lambda(\tau_{\mathrm{p}}^*(60^\circ) - \tau_{60})^2 + (\tau_{\mathrm{p}}^*(0^\circ) - \tau_0)^2 + (\tau_{\mathrm{p}}^*(90^\circ) - \tau_{90})^2, \quad (2)$$

with $\tau_{\mathrm{p}}^*(\phi)$ being the moment produced by the springs, $\lambda = 3, \tau_0 = 20\,\mathrm{Nm}, \tau_{60} = 50\,\mathrm{Nm}, \tau_{90} = 0\,\mathrm{Nm}$. We constrained the attachment points to lie within 60 mm posterior and 50 mm anterior to the shank centerline, and 300 mm inferior and 30 mm superior to the knee joint. Using a trust-region reflective Newton method, we found the optimized attachment points $P : (37, -16)$ and $Q : (-18, -99)$ (coordinate frame of Fig. 2), in combination with two springs with a stiffness of 9.1 kN/m each, and free length of 103 mm. This spring combination allows the motor to stay below twice its nominal torque during level-ground walking. We did not use rubber cords as parallel elastic elements, as it would have required additional force sensing to accurately estimate their joint moment contribution. This is in contrast to the series-elastic elements, where additional force information is available through motor current (Section II-C).

The rocker deflection is measured by a 17 bit absolute encoder (Netzer Precision Motion Sensors Ltd., Misgav, Israel). This angle is used to calculate the deflection of the elastic elements and, hence, the output moment at the knee joint. The same type of encoder is used to measure knee angle. Redundant encoders (14 bit, ams AG, Unterpremstaetten, Austria) are used on the opposite

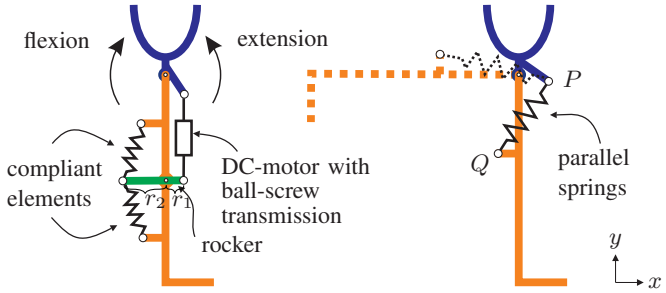

Fig. 2. Conceptual design of the prosthesis with serial (left) and parallel compliant elements (right). Both ideas are incorporated in the prototype (Fig. 4)

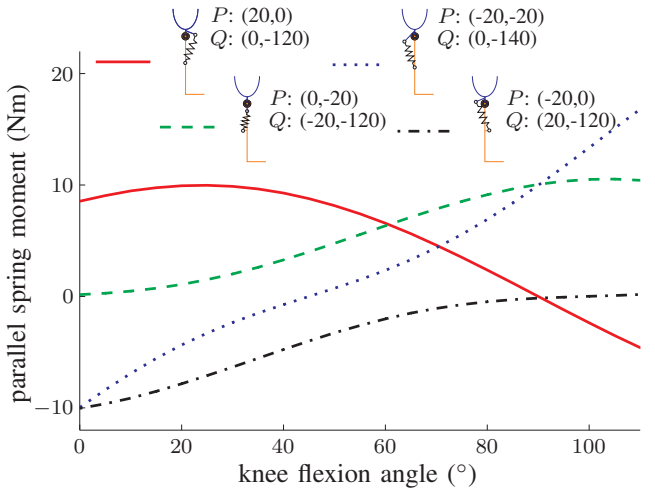

Fig. 3. Knee extension moment produced by a parallel spring assembly ($K = 20\,\mathrm{kN/m}$, $l_0 = 100\,\mathrm{mm}$) for four exemplary attachment points. Coordinates (x, y) for the attachment points are defined in Fig. 2 with the origin at the knee rotation axis (in mm).

side for safety, such that a sensor fault could be detected.

The finalized prototype roughly fits in the outline of a human shank (Fig. 4). The mass of the ANGELAA-leg without the foot is 3.4 kg, and a conventional prosthetic foot approximately adds further 0.7 kg.

C. Knee Moment Observer

A prerequisite for accurate force control is a reliable measurement of joint moment. In a conventional SEA, this moment is directly derived from the deflection of the elastic element, normally a metal spring. However, the rubber cords used here are not ideally elastic, they also have a viscous component. The disadvantages of the viscoelastic elements are hysteresis, caused by a retarded elastic response, as well as creep. To obtain accurate estimates of force despite these two effects, both can be compensated by an observer [42]. Since we did not observe any creep, neither in experiments with this prototype, nor in another robot that uses the same

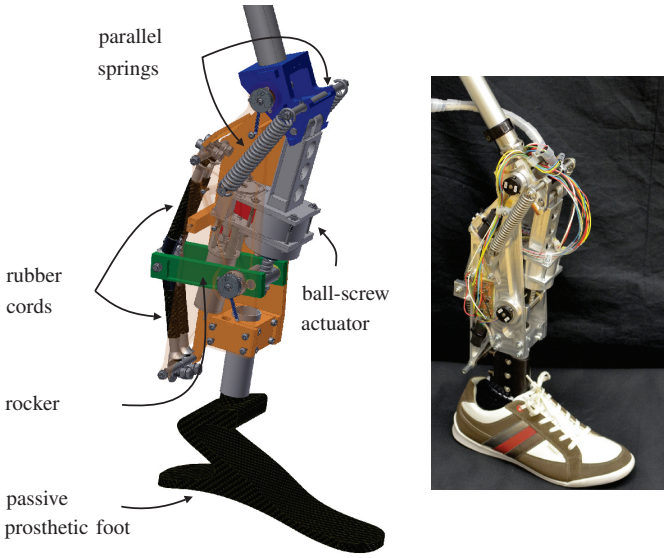

Fig. 4. CAD Drawing of the ANGELAA-leg (left) and picture of finished prototype (right).

rubber cords [43], we simplified the observer to only take retarded elastic response into account.

We selected a model similar to Parietti et al. [42], with a spring and a damper in parallel (a Voigt model), and a spring in series to those two elements. The constitutive equation of the model is

$$\ddot{F} + a\dot{F} = c\ddot{\delta} + d\dot{\delta}, \tag{3}$$

where δ is the deflection of the rocker with respect to the shank, and F is the lumped force of the four rubber cords acting on the rocker. The directions of the forces of the upper and lower cords vary slightly with respect to the rocker, depending on rocker deflection δ. As this dependence is small and has very little effect on the computed knee moment (roughly 0.5 % difference) in the operating range, it was neglected.

In analogy to Parietti et al. [42], the observer combines information on deflection with information on motor torque τ_m, which is calculated from the motor current, as measured by the EPOS3. The motor equation of motion is

$$J_\mathrm{m}\ddot{\varphi}_\mathrm{m} = \tau_\mathrm{m} - \gamma\dot{\varphi}_\mathrm{m} - Fr(\delta, \phi), \tag{4}$$

where $r\,(\delta, \phi)$ denotes the kinematic mapping from rubber cord force F to motor torque τ_m, which depends on the rocker deflection δ and knee angle ϕ, J_m is the lumped inertia of motor and transmission including the rocker, $\dot{\varphi}_\mathrm{m}$ and $\ddot{\varphi}_\mathrm{m}$ are motor velocity and acceleration respectively, and γ is the viscous friction coefficient. After integration, the constitutive equation for the rubber cord force (3) is

$$\dot{F} - \dot{F}_0 + a\,(F - F_0) = c\left(\dot{\delta} - \dot{\delta}_0\right) + d\,(\delta - \delta_0)\,, \tag{5}$$

with the index 0 indicating initial values at time t_0. To simplify notation and without loss of generality, the initial values are assumed to be zero in the following.

Combining the dynamics of the motor (4) and the viscoelastic elements (5), the system can be represented in state-space as

$$\dot{\boldsymbol{x}} = \boldsymbol{A}\boldsymbol{x} + \boldsymbol{B}\boldsymbol{u} + \boldsymbol{w} \quad (6)$$

$$\boldsymbol{y} = \boldsymbol{C}\boldsymbol{x} + \boldsymbol{v}. \quad (7)$$

The state vector $\boldsymbol{x}$, the inputs $\boldsymbol{u}$, and output $\boldsymbol{y}$ are:

$$\boldsymbol{x} = \begin{pmatrix} F - c\delta \\ \varphi_\mathrm{m} \\ \dot{\varphi}_\mathrm{m} \end{pmatrix}, \quad \boldsymbol{u} = \begin{pmatrix} \delta \\ \tau_\mathrm{m} \end{pmatrix}, \quad \boldsymbol{y} = \begin{pmatrix} \varphi_\mathrm{m} \\ \dot{\varphi}_\mathrm{m} \end{pmatrix}.$$

The system matrices are

$$\boldsymbol{A} = \begin{pmatrix} -a & 0 & 0 \\ 0 & 0 & 1 \\ -\frac{r(\delta,\phi)}{J_\mathrm{m}} & 0 & -\frac{\gamma}{J_\mathrm{m}} \end{pmatrix}, \quad \boldsymbol{B} = \begin{pmatrix} d - ac & 0 \\ 0 & 0 \\ -\frac{cr(\delta,\phi)}{J_\mathrm{m}} & \frac{1}{J_\mathrm{m}} \end{pmatrix},$$

$$\boldsymbol{C} = \begin{pmatrix} 0 & 1 & 0 \\ 0 & 0 & 1 \end{pmatrix}.$$

The process noise vector $\boldsymbol{w}$ accounts for dry friction in the rocker, and for backlash. The measurement noise vector $\boldsymbol{v}$ accounts for uncertainties originating from backlash and encoder resolution. A Kalman filter was designed using the covariance matrices of $\boldsymbol{w}$ and $\boldsymbol{v}$, to obtain an estimate $\hat{\boldsymbol{x}}$ of the state vector $\boldsymbol{x}$. The estimate for the rubber cord force $\hat{F}$ is then given by $\hat{F} = \begin{pmatrix} 1 & 0 & 0 \end{pmatrix} \hat{\boldsymbol{x}} + c\delta$, and the estimate for the joint moment is calculated as

$$\hat{\tau} = \hat{F} i(\delta, \phi), \quad (8)$$

where $i(\delta, \phi)$ is the geometric mapping between rubber cord force and joint moment.

D. Communication and Control

All sensor signals are sampled at 1 kHz and collected by an STM32 microcontroller. The signals are communicated at 1 kHz via an RS-485 connection to the xPC Target Realtime computer (Speedgoat GmbH, Liebefeld, Switzerland), which runs the control algorithms at 1 kHz. This allows convenient debugging and fast control design, which was the goal for this tethered prototype. To control the motor, we used the Maxon EPOS3 drive in current control mode and communicating with xPC Target by EtherCAT at 1 kHz.

With the knee moment estimate $\hat{\tau}$ (8), a PI-controller to control knee moment was implemented. The command torque for the motor is

$$\tau_\mathrm{m} = K_\mathrm{P} \left(\tau_\mathrm{ref} - \hat{\tau}\right) + K_\mathrm{I} \int \left(\tau_\mathrm{ref} - \hat{\tau}\right) \mathrm{d}t + \tau_\mathrm{ff}, \quad (9)$$

where τ_ref is the reference knee moment; the controller gains K_P and K_I were tuned manually and were set to $K_\mathrm{P} = 0.014$, $K_\mathrm{I} = 0.014\,\mathrm{s}^{-1}$. Anti-windup limits the integral term in (9) to 1.5 times the motor nominal torque. The feedforward-term is given by $\tau_\mathrm{ff} = \tau_\mathrm{ref} / i_\mathrm{m}(\delta, \phi)$, where $i_\mathrm{m}(\delta, \phi)$ denotes the (configuration-dependent) transmission ratio between motor torque τ_m and knee moment τ.

E. Calibration and Evaluation of Sensing and Control

The parameters in (5) were determined using calibration measurements with a JR3 load cell (JR3 Inc., Woodland, CA, USA). The prosthesis was mounted in horizontal position to eliminate gravitational effects, and it was connected to the load cell with a rope (Fig. 5). The force along the rope was measured and multiplied by its lever arm about the joint, to obtain an accurate measure of the moment for calibration and evaluation.

Measurements were performed at seven different knee angles for extension moments, and seven angles for flexion moments, ranging from 10° to 75° knee angle each. The motor was driven in current control mode to track sinusoidal reference torque profiles, with frequencies ranging from 0.2 Hz to 5 Hz, and amplitudes from 0 to 1.5 times the rated motor torque. The parameters a, c and d in (5) were identified using least-squares optimization from 10 of the 14 datasets. The 4 remaining sets (2 for flexion and 2 for extension) were used to evaluate the accuracy of this moment estimation.

The parameters in (4) were identified using calibration measurements where the rubber cords were removed from the system, so F was equal to zero and the rocker could move freely, detached from the shank. The motor was commanded to follow a sinusoidal reference position trajectory with increasing frequency. Motor acceleration $\ddot{\varphi}_\mathrm{m}$ was obtained by numerical derivation and smoothing (with cut-off frequency of 10 Hz) of the motor velocity $\dot{\varphi}_\mathrm{m}$ measured by the drive. The inertia J_m of the drive train and viscous damping γ were identified using least-squares regression.

To verify the stiffness-angle relationship of the prosthetic knee, we first linearized the identified rubber cords' nonlinear visco-elastic model, to obtain an average estimate for the stiffness over the entire range of knee angles. Then, we determined joint stiffness at the distinct knee angles from the experimental data as follows: From the change in rocker deflection angle $\Delta\delta$, we calculated the equivalent knee angle deflection $\Delta\phi$ if the motor had been been blocked. With the JR3 load cell, we measured the change in knee moment $\Delta\tau$. This yielded a measure of the physical stiffness $K = \Delta\tau / \Delta\phi$ at the corresponding knee angle.

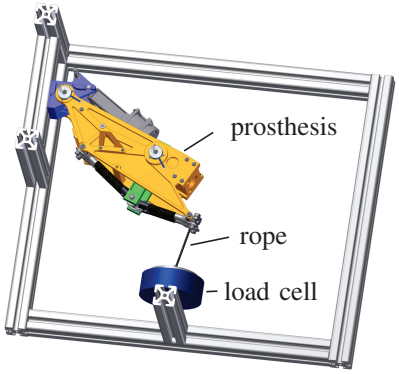

Fig. 5. Setup for moment calibration and evaluation.

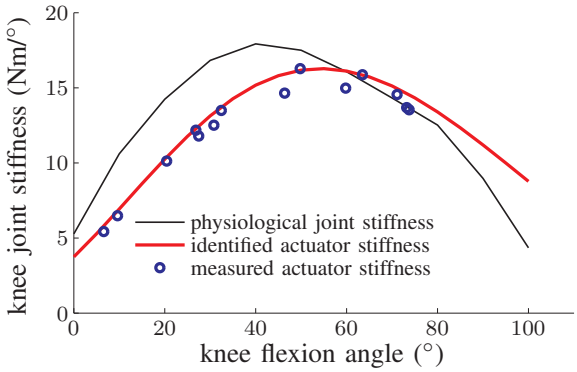

Fig. 6. Identified physical stiffness profile and measured stiffness of the prosthetic joint compared to physiological stiffness requirements (from Fig. 1).

To evaluate force control performance, the device was physically fixed at a knee angle of approximately 50° in horizontal position, similar to Fig. 5, but without the load cell and fixed with pretensioned ropes in both directions. A sinusoidal reference knee moment was commanded with a frequency that slowly increased from 0.2 Hz to 20 Hz, with multiple oscillations for each frequency. The measured moment was then compared to the reference moment in terms of phase lag and amplification in steady state for each frequency. This experiment was repeated at different amplitudes ranging from 5 Nm to 30 Nm.

All experiments in the test setup were performed without the prosthetic foot and without the parallel springs, as we wanted to focus on the behavior of the serial springs, and the contribution of the parallel springs to stiffness was negligible (see Section III-A).

F. Pilot Walking Experiment

We performed a pilot experiment with a unilateral transfemoral amputee (age 44, height 186 cm, weight 75 kg). A Vari-Flex passive foot (Össur, Reykjavik, Iceland) was used. The experiment was approved by the Ethics Committee of the Canton of Zurich.

We employed a finite-state controller as commonly done in active transfemoral prostheses [4], [6], [18], where we divided a gait cycle into four states associated with different impedance parameters. The control law in each state can be described as

$$\tau_{\text{ref}} = K\left(\phi - \phi_0\right) - B\dot{\phi}, \tag{10}$$

where K represents virtual stiffness with setpoint ϕ_0, and B virtual damping. These three parameters, as well as the switching conditions between the four states, were tuned manually.

The subject walked on a treadmill at a self-selected speed of 2.2 km/h for about 10 minutes (after 5 minutes familiarization time on even ground with hand rails), with short breaks to tune controller parameters. The final parameters are reported in Table I. Using these parameters, we recorded knee angle, as well as reference and actual knee moments of the prosthesis at 1 kHz, to assess moment tracking performance.

State	K (Nm/°)	ϕ_0 (°)	B (Nms/°)	transition condition
1	2.6	8	0.02	$\phi > 10\,° \;\&\; \dot{\phi} > 5.7\,°/\text{s}$
2	1.4	7	0	$\phi > 20\,° \;\&\; \dot{\phi} > 5.7\,°/\text{s}$
3	0.9	70	0	$\phi > 50\,° \;\&\; \dot{\phi} < 0\,°/\text{s}$
4	0	20	0.02	$\phi < 15\,°$

TABLE I
PARAMETERS OF THE IMPEDANCE CONTROLLER. WHEN THE INDICATED TRANSITION CONDITION IS FULFILLED, THE CONTROLLER SWITCHES TO THE NEXT STATE IN THE TABLE (EXCEPT FROM 4 IT SWITCHES BACK TO 1).

III. Results

A. Physiological and Replicated Stiffness and Moment

The physical stiffness of ANGELAA as a function of knee angle closely approximates the physiological stiffness over the entire angle range (Fig. 6). The peak physical stiffness of approximately 16 Nm/° is reached at 55° knee angle, and it decreases towards 4 Nm/° near full extension and towards 6 Nm/° for full flexion. Compared to the stiffness of the serial springs, the additional stiffness gained by the parallel springs (not included in the figure), defined as the derivative of knee moment with respect to angle, is almost negligible ($< 0.5\,\text{Nm}/°$ for the whole range of motion).

The peak moment characteristics of the chosen hardware configuration (given that the motor can be overloaded to up to four times its nominal torque) are shown in Fig. 7. The peak moments that actuator and parallel springs can produce are substantially lower than what a physiological knee is capable of (Fig. 7). The theoretical

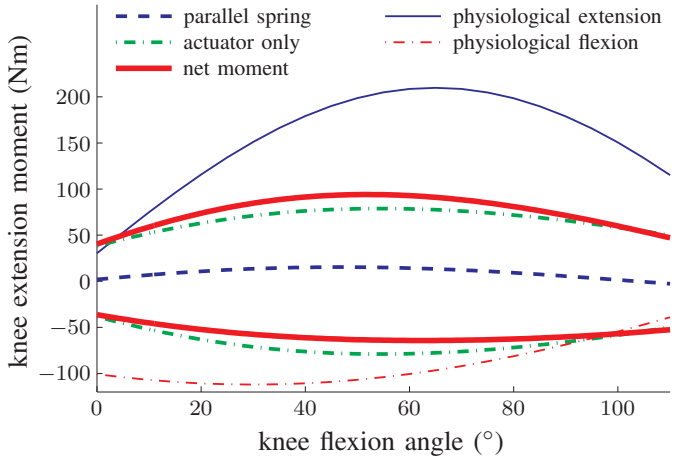

Fig. 7. Peak moment profile of the prosthetic joint compared to physiological moment requirements, assuming a motor peak torque of 4 times its nominal torque. The parallel springs lead to a net joint moment that is biased in extension direction (solid red line).

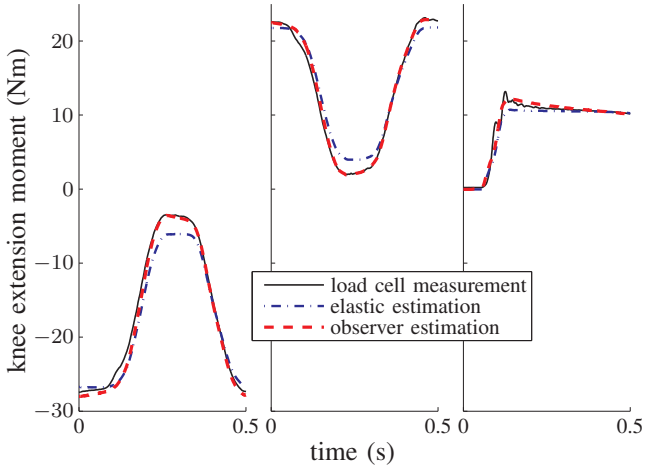

Fig. 8. Comparison of moment estimates to moment measurement from a load cell for two typical 2 Hz oscillations (flexion in the left plot, extension in the middle plot), and an impact-like situation where the rope was not under tension in the beginning (right plot). The dash-dotted line represents a simple elastic model that does not consider viscoelastic effects, and the dashed line represents the observer estimates (Eq. (8)).

peak moment that can be reached is 94 Nm at a knee flexion angle of 53°, where the actuator delivers 79 Nm and the parallel spring 15 Nm (an increase of 19 %). The contribution of the parallel springs approaches 0 Nm near full knee extension and knee flexion.

B. Benefit of Angle-Dependent Stiffness Requirements

To quantify the benefit of an angle-dependent stiffness requirement, we compared our design (with the identified stiffness from Fig. 6) to a hypothetical design that fulfills maximum stiffness requirements independent of knee angle. This hypothetical design uses the same geometry and actuation principle from Section II-B. For this design, we require the stiffness to be at least 16 Nm/° (the peak value achieved by our actuator, see Fig. 6), regardless of joint angle. Based on the notion introduced above, saying that the physical stiffness, reflected on the knee joint, must be at least as high as the maximum required stiffness [20], we selected the stiffness of the series elastic springs such that the maximum joint stiffness could be achieved independent of knee angle. This resulted in an increase of the series spring stiffness by a factor of 4.3, which transfers to an increased joint stiffness K by the same factor (yielding a peak of approximately 70 Nm/°).

An upper bound for the impedance that can be reached by a SEA in zero-force control is the intersection of the impedance of the end-effector inertia J_e (with impedance $Z(j\omega) = j\omega J_e$) and the series stiffness K (with impedance $Z(j\omega) = K/(j\omega)$), assuming resonance can be prevented by the controller [20]. The value of the impedance at this intersection is given by $Z = \sqrt{KJ_e}$. So if joint stiffness K is 4.3 times as high as in our design, the upper bound for the impedance increases by factor $\sqrt{4.3}$. This means exploitation of our angle-dependent stiffness requirement leads to an improvement in force tracking approximately by factor two.

C. Moment Measurement

The nonlinear viscoelastic model (5) approximated the actual knee moment with a coefficient of determination R^2 of 0.993. Fig. 8 shows two of the four validation measurements, and an impact-like situation where the rope was not under tension at the beginning of the measurement. The identified parameter values of the model were $a = 5.47\,\mathrm{s}^{-1}$, $c = 23.8\,\mathrm{N/°}$, and $d = 108.7\,\mathrm{N/(s{\cdot}°)}$, and the parameters in (4) were $J = 1.54 \cdot 10^{-5}\,\mathrm{kg \cdot m^2}$ and $\gamma = 4.20 \cdot 10^{-4}\,\mathrm{kg \cdot m^2/s}$. Maximum dry friction was 0.025 Nm. The measurements revealed an average absolute error of 0.73 Nm over the four test data sets. Due to the nonlinearity of the kinematics and the slight nonlinearity of the rubber cords' force characteristics, the moment resolution depends on the knee angle and on the exerted moment; it ranged from 0.003 Nm at zero knee moment and 60° knee angle, to 0.013 Nm at 50 Nm knee moment and 10° knee angle.

D. Bandwidth

The moment bandwidth of the prosthetic joint decreased with increasing amplitude, reaching 9 Hz at 5 Nm, and 5 Hz at 30 Nm (Fig. 9).

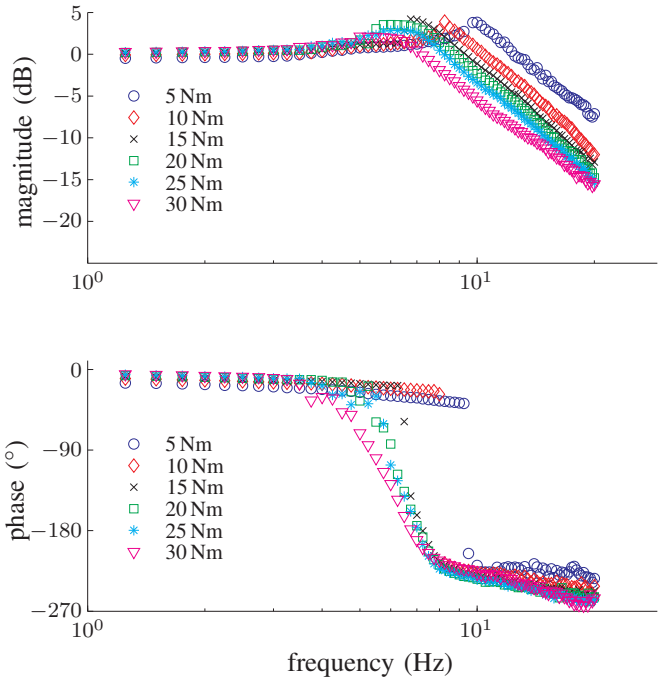

Fig. 9. Experimental tracking frequency response of the prosthesis for different moment amplitudes. The data points indicate the steady-state response at the corresponding frequency.

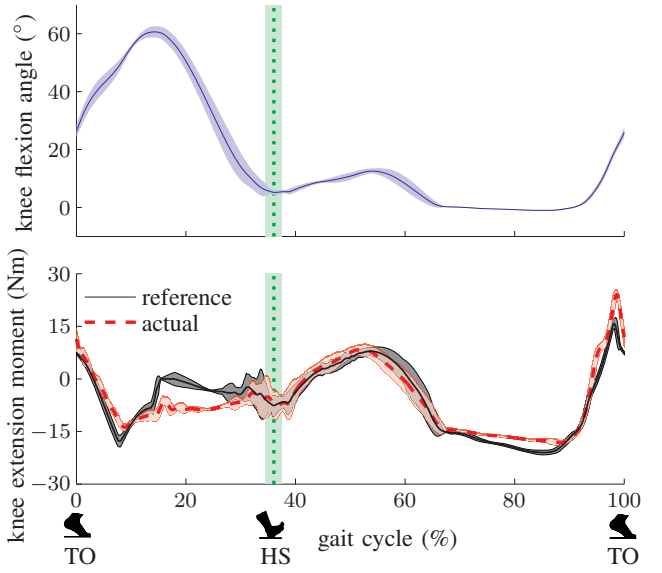

Fig. 10. Moment tracking performance: reference knee moment and actual knee moment as measured by the observer in an amputee experiment during treadmill walking. Mean and standard deviation (shaded areas) are shown over 10 gait cycles. Cycles are plotted from toe-off (TO) to toe-off, to highlight the performance during heel-strike (HS, green dashed line).

E. Pilot Walking Experiment

The amputee was able to walk with the simple switching controller on a treadmill after very little familiarization time (less than 5 minutes). The controller tracked the reference moment accurately throughout most of the gait cycle, with less accurate tracking during swing phase (Fig. 10). It should be highlighted that the impact situation at heel strike did not pose any problem for the controlled actuator.

IV. Discussion

Our goal was to design a tethered transfemoral prosthesis that can mimic the capabilities of a physiological knee joint in terms of stiffness, moment generation and velocity, so that it can serve as a research platform for control design and evaluation.

Compared to variable-stiffness actuators, our proposed concept does not include a second actuator to adjust the physical stiffness, but the change of physical stiffness is directly coupled to joint angle. The requirements for the relationship between joint angle and stiffness are obtained by conducting a precise analysis of physiological stiffness-angle relationships. To our knowledge, ANGELAA is the first device specifically designed to replicate physiological knee stiffness, which was possible using our recently developed approach to estimate physiological knee stiffness [17]. We have shown that the upper bound for the impedance in zero-force control could be reduced by a factor of two when using the angle-dependent stiffness requirement, compared to a design that would consider only the maximum stiffness independent of knee angle.

Theoretically, it would be possible to realize a construction with a physical stiffness that is constant over the entire angle range and equal to the required peak stiffness. That could for example employ a rotary spring in the joint. Such a construction is more difficult to realize, and it would sacrifice force control performance in areas in the workspace where high joint stiffness is not needed.

The optimized geometry for the SVA enabled ANGELAA to cover the required physical stiffness almost completely (Fig. 6). In addition, the placement of the parallel springs was able to augment the moment generated by the motor by almost 20 % at knee angles where high extension moments are needed (Fig. 7).

The peak joint moments of the human knee joint could not be achieved with the given weight constraints. Still, the device should be usable for common locomotor abilities such as stair climbing: Literature data from able-bodies subjects suggests that peak knee extension moments during stair climbing do not exceed 1.1 Nm/kg [30]. Assuming a transfemoral prosthesis that can ideally replicate physiological gait (including an actuated ankle), our prototype would allow stair climbing

for subjects of 85 kg, although our requirements were based on only 75 kg body mass. In the case of a passive foot, required knee moments are likely much lower; it has been shown that transtibial amputees with a passive foot prosthesis - a situation comparable to our configuration of a powered knee with a passive ankle prosthesis - need much lower knee moments during stair ambulation [31] than able-bodied subjects.

The position of the parallel springs was optimized to increase net extension moment where physiological extension moments are highest, which in turn reduces the achievable peak flexion moments. This reduction is acceptable, as flexion moments during physiological locomotion are comparably small (Fig. 7). However, for a self-contained device, it might be better to optimize for low power consumption. The mass of the parallel springs is low (84 g per spring) compared to the mass of the device (3.4 kg), but if the goal is not to replicate the asymmetric moment capabilities, and a motor with similar energy density can be found, a heavier motor could be used to achieve higher knee moments. The parallel springs produce only negligible joint moments near 0° and 90° knee flexion angle, angles required for standing and sitting respectively. This is highly desirable, because it creates natural equilibria and ensures that the actuator does not need to counteract the parallel springs in these frequent postures.

It should be noted that during level-ground walking of able-bodied subjects, the knee joint only generates little positive kinetic energy [29], [30], and entirely passive joints may be suitable for prosthetic or orthotic devices aiming to restore physiological gait, as investigated by several research groups [44]–[47]. Nevertheless, it has been shown that powered knees can decrease metabolic energy consumption during level-ground walking [48]. Other tasks such as climbing stairs in a physiological way rely on positive energy from the knee joint, which requires a powered device.

Our prototype does not include an actuated foot, which would be necessary to restore a completely natural gait pattern. A powered knee with a passive foot can theoretically bring a transfemoral amputee to the level of a transtibial amputee with a passive foot; transtibial amputees have been shown to have better walking abilities than transfemoral amputees [49]. Another approach would be a passive knee combined with an actuated foot [16], which might help in level-ground walking, but will likely still limit activities such as stair climbing or sit-to-stand transfer.

The mass of the device is similar to the mass of an adult human leg. It is 4.1 kg (including a passive foot), which corresponds to a foot and shank mass of a 67 kg human [29]. About 20 % of the American males aged 20-29 are lighter, as are about 10 % of the 30-79 year old [50]. The weight is comparable to other powered devices [4], [5], [7], but substantially heavier than variable-damping devices such as the C-Leg by Otto Bock, which weighs around 1.2 kg (without foot). It was not our focus to minimize the weight of this prototype, and there is potential to optimize structure and materials to reduce the weight substantially; the employed mechatronic principles do not prohibit a more lightweight design. However, an active prosthesis will always be heavier than a passive one, and future experiments with patients will show whether the benefits of a powered knee joint outweigh the disadvantage of additional weight. It should be noted that it is unclear which weight is acceptable for a transfemoral prosthesis. While it is often stated that it should be as lightweight as possible due to the delicate interface between residual limb and shaft, which is also our experience with clinical partners, there is evidence in the literature that patients do not necessarily prefer the most lightweight devices, at least in passive knee joints [51], [52].

In terms of length, the current prototype with a high-profile foot can be made as long as necessary by using different aluminum tubes, and as short as 0.44 m (measured from rotation axis to the floor); only 1 percent of the American male population has shorter shanks [53]. For knee-exarticulated amputees, the prosthesis has to be shorter than the physiological shank, in which case, depending on their shank length, a low-profile prosthetic foot would have to be employed.

Our device achieved a bandwidth of $\sim$ 5 Hz for a sinusoidal oscillation with an amplitude of 30 Nm. When defining the physiological moment bandwidth as the frequency range over which 70 % of the signal is captured (analog to Au and Herr [36]), the physiological knee moment bandwidth was found to be approximately 4 Hz, where knee torque varied between 0 and 35 Nm (based on data from Riener et al. [30]). Therefore, the device should provide sufficient bandwidth.

Our approach to estimate physiological stiffness, which formed the basis for the formulation of requirements, has so far been validated by comparison to isometric perturbation experiments [17]. It has not yet been validated during gait, because it is very difficult to apply perturbations to the joint without impeding natural gait. Literature suggests that stiffness during movement could be lower than what would be expected from observations in the static case, for example, in the elbow joint [54]. It has also been observed that joint stiffness decreases during movement onset [55], [56]. Future perturbation experiments during gait will show how well our approach

estimates stiffness in locomotor activities [13].

In contrast to conventional SEAs, we used viscoelastic rubber cords instead of regular springs. The rubber cords have two main advantages over regular steel springs. First, they provide intrinsic damping, which allows the use of higher controller gains and, hence, more accurate and robust force control [40]–[42]. Second, they are lighter than steel springs of comparable stiffness, allowing for lighter designs that put less strain on the stump. The commonly stated disadvantages connected with viscoelasticity, in particular hysteresis, did not impede our moment sensing: Experimental evaluation showed that our observer structure allowed precise and accurate estimates of joint moment (roughly 1 % of the peak moment of the device). We did not encounter any disadvantages of the rubber cords, other than a minor increase in computational effort to estimate knee moment and a mechanically slightly more complex fixation compared to regular steel springs. To clearly decide whether the benefits (light weight and added viscosity) outweigh these disadvantages, experimental comparison to regular steel springs may be required.

While we did not assess long-term effects when using these rubber cords, we did not observe any changing behavior with prolonged use of the rubber cords neither in this prototype nor in another robot [43]. Should their properties change over time, this could be detected by comparing rubber deflection and motor torque over time, and the cords should be replaced.

In the amputee experiment we focused on moment tracking performance. Hence, little time was spent on tuning the parameters of the switching controller, and a more extensive tuning may improve gait characteristics. Furthermore, we used a passive foot, which inherently limits reproduction of physiological gait compared to devices including an actuated ankle [5]. Finally, it should be noted that the amputee walked at a self-selected speed of 2.2 km/h, which is relatively slow (compared to 2.9-4.2 km/h reported in [57]), and it would be interesting to investigate higher speeds in the future.

V. Conclusion

In this proof-of-concept, we presented a new variant of Series-(Visco-)Elastic Actuator that changes its physical stiffness in function of kinematic configuration, optimized to mimic physiology. The concept was used in a prototype of a transfemoral prosthesis (the ANGELAA-leg), and the required stiffness (and moment) profiles were derived from precise analysis of physiological capabilities. Two further design features reduce weight: rubber cords as series-elastic elements, and nonlinear parallel elasticity to reduce motor torque requirements. The mechatronic principles described in this paper can be transferred to other impedance-controlled devices where stiffness requirements can be specified in advance and formulated in function of kinematic configuration, and where weight, cost, or power consumption are critical. Examples are other wearable devices like ankle prostheses or leg exoskeletons, but also mobile manipulators.

Acknowledgment

The authors would like to thank U. Keller, M. Tucker and P. Lutz for their valuable input during the design phase, and E. J. Perrault and M. Hardegger for their work and support with the stiffness-estimation model. They also thank the technical staff P. Wespe, A. Rotta, M. Bader and M. Herold-Nadig for their effort and help during manufacturing and system integration, and M. Hofer and S. Bühler for their help with the amputee experiment.

References

[1] B. J. Hafner, L. L. Willingham, N. C. Buell, K. J. Allyn, and D. G. Smith, "Evaluation of function, performance, and preference as transfemoral amputees transition from mechanical to microprocessor control of the prosthetic knee," *Arch. Phys. Med. Rehabil.*, vol. 88, no. 2, pp. 207 – 217, 2007.

[2] M. Schaarschmidt, S. W. Lipfert, C. Meier-Gratz, H.-C. Scholle, and A. Seyfarth, "Functional gait asymmetry of unilateral transfemoral amputees," *Hum Movement Sci*, vol. 31, no. 4, pp. 907–917, 2012.

[3] M. Bellmann, T. Schmalz, E. Ludwigs, and S. Blumentritt, "Immediate effects of a new microprocessor-controlled prosthetic knee joint: A comparative biomechanical evaluation," *Arch. Phys. Med. Rehabil.*, vol. 93, no. 3, pp. 541 – 549, 2012.

[4] E. C. Martinez-Villalpando and H. Herr, "Agonist-antagonist active knee prosthesis: A preliminary study in level-ground walking," *J. Rehabil. Res. Dev.*, vol. 46, no. 3, pp. 361–374, 2009.

[5] B. Lawson, H. Varol, A. Huff, E. Erdemir, and M. Goldfarb, "Control of stair ascent and descent with a powered transfemoral prosthesis," *IEEE Trans. Neural Syst. Rehabil. Eng.*, vol. 21, no. 3, pp. 466–473, 2013.

[6] B. G. A. Lambrecht and H. Kazerooni, "Design of a semi-active knee prosthesis," in *IEEE Int Conf Robot Autom (ICRA)*, 2009, pp. 639–645.

[7] C. Hoover, G. Fulk, and K. Fite, "Stair ascent with a powered transfemoral prosthesis under direct myoelectric control," *IEEE/ASME Trans. Mechatronics*, vol. 18, no. 3, pp. 1191–1200, 2013.

[8] M. Eilenberg, H. Geyer, and H. Herr, "Control of a powered ankle & foot prosthesis based on a neuromuscular model," *IEEE Trans. Neural Syst. Rehabil. Eng.*, vol. 18, no. 2, pp. 164 –173, april 2010.

[9] A. M. Simon, N. P. Fey, S. B. Finucane, R. D. Lipschutz, and L. J. Hargrove, "Strategies to reduce the configuration time for a powered knee and ankle prosthesis across multiple ambulation modes," in *Conf. Proc. IEEE Int. Conf. Rehabil. Robot. (ICORR)*, 2013.

[10] S. Song and H. Geyer, "Regulating speed and generating large speed transitions in a neuromuscular human walking model," in *IEEE Int Conf Robot Autom (ICRA)*, 2012, pp. 511–516.

[11] E. Rouse, L. Hargrove, E. Perreault, and T. Kuiken, "Estimation of human ankle impedance during the stance phase of walking," *IEEE Trans Neural Syst Rehabil Eng*, no. 99, 2014, in press.

[12] H. Lee and N. Hogan, "Investigation of human ankle mechanical impedance during locomotion using a wearable ankle robot," in *IEEE Int Conf Robot Autom (ICRA)*, 2013, pp. 2636–2641.

[13] M. Tucker, A. Moser, O. Lambercy, J. Sulzer, and R. Gassert, "Design of a wearable perturbator for human knee impedance estimation during gait," in *Conf. Proc. IEEE Int. Conf. Rehabil. Robot. (ICORR)*, 2013.

[14] P. M. H. Rack and D. R. Westbury, "The short range stiffness of active mammalian muscle and its effect on mechanical properties," *J. Physiol.*, vol. 240, no. 2, pp. 331–350, 1974.

[15] E. Rouse, R. Gregg, L. Hargrove, and J. Sensinger, "The difference between stiffness and quasi-stiffness in the context of biomechanical modeling," *IEEE Trans. Biomed. Eng.*, vol. 60, no. 2, pp. 562–568, 2013.

[16] J. Geeroms, L. Flynn, R. Jimenez-Fabian, B. Vanderborght, and D. Lefeber, "Ankle-knee prosthesis with powered ankle and energy transfer for CYBERLEGs α-prototype." in *Conf. Proc. IEEE Int. Conf. Rehabil. Robot. (ICORR)*, 2013.

[17] S. Pfeifer, H. Vallery, M. Hardegger, R. Riener, and E. J. Perreault, "Model-based estimation of knee stiffness," *IEEE Trans. Biomed. Eng.*, vol. 59, no. 9, pp. 2604 –2612, sept. 2012.

[18] F. Sup, H. A. Varol, J. Mitchell, T. J. Withrow, and M. Goldfarb, "Preliminary evaluations of a self-contained anthropomorphic transfemoral prosthesis," *IEEE/ASME Trans. Mechatronics*, vol. 14, no. 6, pp. 667–676, 2009.

[19] A. Albu-Schaffer, O. Eiberger, M. Grebenstein, S. Haddadin, C. Ott, T. Wimbock, S. Wolf, and G. Hirzinger, "Soft robotics," *IEEE Robot. Autom. Mag.*, vol. 15, no. 3, pp. 20 –30, 2008.

[20] H. Vallery, J. Veneman, E. van Asseldonk, R. Ekkelenkamp, M. Buss, and H. van der Kooij, "Compliant actuation of rehabilitation robots," *IEEE Robot. Autom. Mag.*, vol. 15, no. 3, pp. 60–69, 2008.

[21] N. Paine, S. Oh, and L. Sentis, "Design and control considerations for high-performance series elastic actuators," *IEEE/ASME Trans. Mechatronics*, vol. 19, no. 3, pp. 1080–1091, June 2014.

[22] Y. Kim, J. Lee, and J. Park, "Compliant joint actuator with dual spiral springs," *IEEE/ASME Trans. Mechatronics*, vol. 18, no. 6, pp. 1839–1844, Dec 2013.

[23] M. Hutter, C. Remy, M. Hoepflinger, and R. Siegwart, "Efficient and versatile locomotion with highly compliant legs," *IEEE/ASME Trans. Mechatronics*, vol. 18, no. 2, pp. 449–458, April 2013.

[24] S. Stramigioli, G. van Oort, and E. Dertien, "A concept for a new energy efficient actuator," in *IEEE Int. Conf. Adv. Intel. Mech. (AIM)*, july 2008, pp. 671 –675.

[25] A. Jafari, N. Tsagarakis, I. Sardellitti, and D. Caldwell, "A new actuator with adjustable stiffness based on a variable ratio lever mechanism," *IEEE/ASME Trans. Mechatronics*, vol. 19, no. 1, pp. 55–63, Feb 2014.

[26] B. Vanderborght, N. Tsagarakis, C. Semini, R. Van Ham, and D. Caldwell, "MACCEPA 2.0: Adjustable compliant actuator with stiffening characteristic for energy efficient hopping," in *IEEE Int Conf Robot Autom (ICRA)*, 2009, pp. 544–549.

[27] S. Groothuis, G. Rusticelli, A. Zucchelli, S. Stramigioli, and R. Carloni, "The variable stiffness actuator vsaut-ii: Mechanical design, modeling, and identification," *IEEE/ASME Trans. Mechatronics*, vol. 19, no. 2, pp. 589–597, April 2014.

[28] S. Bédard and P.-O. Roy, "Actuated leg prosthesis for above-knee amputees," US Patent US7 314 490, 2008.

[29] D. A. Winter, *Biomechanics and Motor Control of Human Movement*, 2nd ed. New York: Wiley, 1990.

[30] R. Riener, M. Rabuffetti, and C. Frigo, "Stair ascent and descent at different inclinations," *Gait & Posture*, vol. 15, no. 1, pp. 32–44, 2002.

[31] T. Schmalz, S. Blumentritt, and B. Marx, "Biomechanical analysis of stair ambulation in lower limb amputees," *Gait & Posture*, vol. 25, no. 2, pp. 267–278, 2007.

[32] M. Alimusaj, L. Fradet, F. Braatz, H. J. Gerner, and S. I. Wolf, "Kinematics and kinetics with an adaptive ankle foot system during stair ambulation of transtibial amputees," *Gait & Posture*, vol. 30, no. 3, pp. 356 – 363, 2009.

[33] D. E. Anderson, M. L. Madigan, and M. A. Nussbaum, "Maximum voluntary joint torque as a function of joint angle and angular velocity: Model development and application to the lower limb," *J. Biomech.*, vol. 40, no. 14, pp. 3105–13, 2007.

[34] M. E. Houston, R. W. Norman, and E. A. Froese, "Mechanical measures during maximal velocity knee extension exercise and their relation to fibre composition of the human vastus lateralis muscle," *European Journal of Applied Physiology and Occupational Physiology*, vol. 58, no. 1-2, pp. 1–7, 1988.

[35] A. Zoss and H. Kazerooni, "Design of an electrically actuated lower extremity exoskeleton," *Advanced Robotics*, vol. 20, no. 9, pp. 967–988, 2006.

[36] S. Au and H. Herr, "Powered ankle-foot prosthesis," *IEEE Robot. Autom. Mag.*, vol. 15, no. 3, pp. 52 –59, 2008.

[37] J. Sensinger and R. Weir, "Design and analysis of a non-backdrivable series elastic actuator," in *Conf. Proc. IEEE Int. Conf. Rehabil. Robot. (ICORR)*, 2005, pp. 390–393.

[38] S. Wang, C. Meijneke, and H. van der Kooij, "Modeling, design, and optimization of mindwalker series elastic joint," in *Conf. Proc. IEEE Int. Conf. Rehabil. Robot. (ICORR)*, vol. 2013, 2013, pp. 1–8.

[39] S. Pfeifer, R. Riener, and H. Vallery, "An actuated transfemoral prosthesis with optimized polycentric knee joint," in *IEEE/RAS-EMBS Int. Conf. Biomed. Robot. Biomechatronics (BioRob)*, june 2012, pp. 1807 –1812.

[40] J. W. Hurst, D. Hobbelen, and A. Rizzi, "Series elastic actuation: Potential and pitfalls," in *Conf. Proc. Int. Conf. on Climbing and Walking Robots*, 2004.

[41] J. Oblak and Z. Matjacic, "Design of a series visco-elastic actuator for multi-purpose rehabilitation haptic device," *J. Neuroeng. Rehabil.*, vol. 8, no. 1, p. 3, 2011.

[42] F. Parietti, G. Baud-Bovy, E. Gatti, R. Riener, L. Guzzella, and H. Vallery, "Series viscoelastic actuators can match human force perception," *IEEE/ASME Trans. Mechatronics*, vol. 16, no. 5, pp. 853–860, 2011.

[43] H. Vallery, P. Lutz, J. von Zitzewitz, G. Rauter, M. Fritschi, C. Everarts, R. Ronsse, A. Curt, and M. Bolliger, "Multidirectional transparent support for overground gait training," in *Conf. Proc. IEEE Int. Conf. Rehabil. Robot. (ICORR)*, 2013.

[44] R. Unal, S. Behrens, R. Carloni, E. Hekman, S. Stramigioli, and H. Koopman, "Prototype design and realization of an innovative energy efficient transfemoral prosthesis," in *IEEE/RAS-EMBS Int. Conf. Biomed. Robot. Biomechatronics (BioRob)*, sept. 2010, pp. 191 –196.

[45] A. Matthys, P. Cherelle, M. Van Damme, B. Vanderborght, and D. Lefeber, "Concept and design of the HEKTA (harvest energy from the knee and transfer it to the ankle) transfemoral prosthesis," in *IEEE/RAS-EMBS Int. Conf. Biomed. Robot. Biomechatronics (BioRob)*, june 2012, pp. 550 –555.

[46] E. Wentink, H. Koopman, S. Stramigioli, J. Rietman, and P. Veltink, "Variable stiffness actuated prosthetic knee to restore knee buckling during stance: A modeling study," *Med. Eng. Phys.*, vol. 35, no. 6, pp. 838 – 845, 2013.

[47] T. Bulea, R. Kobetic, C. To, M. Audu, J. Schnellenberger, and R. Triolo, "A variable impedance knee mechanism for controlled stance flexion during pathological gait," *IEEE/ASME Trans. Mechatronics*, vol. 17, no. 5, pp. 822–832, 2012.

[48] E. Martinez-Villalpando, L. Mooney, G. Elliott, and H. Herr, "Antagonistic active knee prosthesis. a metabolic cost of walking comparison with a variable-damping prosthetic knee," in *Conf Proc IEEE Eng Med Biol Soc (EMBC)*, 30 2011-sept. 3 2011, pp. 8519 –8522.

[49] W. C. Miller, M. Speechley, and B. Deathe, "The prevalence and risk factors of falling and fear of falling among lower extremity amputees," *Archives of Physical Medicine and Rehabilitation*, vol. 82, no. 8, pp. 1031 – 1037, 2001.

[50] "U.s. census bureau, statistical abstract of the united states: 2012."

[51] R. W. Selles, J. B. Bussmann, R. C. Wagenaar, and H. J. Stam, "Effects of prosthetic mass and mass distribution on kinematics and energetics of prosthetic gait: A systematic review," *Arch. Phys. Med. Rehabil.*, vol. 80, no. 12, pp. 1593–99, 1999.

[52] B. Meikle, C. Boulias, T. Pauley, and M. Devlin, "Does increased prosthetic weight affect gait speed and patient preference in dysvascular transfemoral amputees?" *Arch. Phys. Med. Rehabil.*, vol. 84, no. 11, pp. 1657–61, 2003.

[53] A. R. Tilley, *The Measure of Man and Woman*, R. de Alba, Ed. Henry Dreyfuss Associates, 1993.

[54] D. Bennett, J. Hollerbach, Y. Xu, and I. Hunter, "Time-varying stiffness of human elbow joint during cyclic voluntary movement," *Exp. Brain Res.*, vol. 88, pp. 433–442, 1992.

[55] D. Ludvig, S. Antos, and E. Perreault, "Joint impedance decreases during movement initiation," in *Conf Proc IEEE Eng Med Biol Soc (EMBC)*, 28 2012-sept. 1 2012, pp. 3304 –3307.

[56] J. B. MacNeil, R. E. Kearney, and I. W. Hunter, "Identification of time-varying biological systems from ensemble data (joint dynamics application)," *IEEE Trans. Biomed. Eng.*, vol. 39, no. 12, pp. 1213 –1225, dec. 1992.

[57] T. Schmalz, S. Blumentritt, and R. Jarasch, "Energy expenditure and biomechanical characteristics of lower limb amputee gait: The influence of prosthetic alignment and different prosthetic components," *Gait & Posture*, vol. 16, no. 3, pp. 255–263, 2002.

Serge Pfeifer Serge Pfeifer studied electrical engineering and information technology at ETH Zurich, ETH Lausanne and at the University of Edinburgh. In 2008 he received his Master's degree. In 2014, he was awarded his PhD degree by ETH Zürich. He was a visiting researcher at the Rehabilitation Institute of Chicago in 2011. His work focuses on estimating biological knee stiffness and transferring such concepts to the design of powered transfemoral prostheses. His patent application on a powered prosthesis with serial and/or parallel compliance was selected among the 20 best inventions of ETH Zurich in 2013.

Anna Pagel Anna Pagel received her Dipl.-Ing. degree in mechanical engineering from Karlsruhe Institute of Technology in 2010. Since 2011, she is a doctoral student with the Sensory-Motor Systems Lab, ETH Zurich, Switzerland. Her research focuses on sensory augmentation, joint impedance identification and user-cooperative control strategies for actuated knee exoprostheses.

Robert Riener Robert Riener studied mechanical engineering at TU München, Munich, Germany, and University of Maryland, College Park. He received a Ph.D. degree in engineering from the TU München, in 1997. Currently, he is full professor for Sensory-Motor Systems at the Department of Health Sciences and Technology, ETH Zurich, and professor of medicine at the University Clinic Balgrist, University of Zurich. Riener has published more than 400 peer-reviewed journal and conference articles, 20 books and book chapters and filed 20 patents. He has received more than 15 personal distinctions and awards including the Swiss Technology Award in 2006, the IEEE TNSRE Best Paper Award 2010, and the euRobotics Technology Transfer Awards 2011 and 2012. Riener's research focuses on the investigation of the sensory-motor actions in and interactions between humans and machines. This includes the study of human sensory-motor control, the design of novel user-cooperative robotic devices and virtual reality technologies, and the investigation and optimisation of human-machine interaction. Main application areas are the fields of rehabilitation and sports.

Heike Vallery Heike Vallery received the Dipl.-Ing. degree in Mechanical Engineering from RWTH Aachen University in 2004, and she received her PhD from Technische Universität München in 2009. As a postdoc at ETH Zürich, she established a research group on leg exoprosthetics. Currently, she holds an assistant professorship at Delft University of Technology, and she also remains affiliated with ETH. Her research interests are in the areas of bipedal locomotion, compliant actuation, and rehabilitation robotics. She has published more than 40 peer-reviewed publications, filed 4 patents, and received diverse fellowships and awards, most recently the 1st prize of the euRobotics Technology Transfer Award 2014.